Medicinal Plant Biology

ARTICLE

Open Access

https://doi.org/10.48130/mpb-0026-0015

Medicinal Plant Biology **2026**, 5: e019

The influence of different processing methods on the quality and pharmacological effects of harvested *Corydalis Rhizoma*

Hui Yang[1#], Baicheng Li[1#], Zhuoke Li[1#], Hongwen Zhao[1], Na Zheng[2], Junfeng Liu[1], Hong Zhang[1*] and Tingting Sun[1*]

[1] *Shaanxi Academy of Traditional Chinese Medicine (Shaanxi Hospital of Traditional Chinese Medicine), Xi'an 710003, China*

[2] *School of Life Science, Northwest University, Xi'an 710069, China*

[#] Authors contributed equally: Hui Yang, Baicheng Li, Zhuoke Li

* Correspondence: zhanghong919919@163.com (Zhang H); sttlt@126.com (Sun T)

Abstract

Corydalis Rhizoma (CR) is commonly used as an analgesic herb in Traditional Chinese Medicine. Conventional processing requires repeated soaking and softening, which accelerates the loss of water-soluble active ingredients and reduces efficacy. This study developed a fresh-cut processing technique to reduce costs, shorten processing time, and improve CR quality and efficacy. Initially, the fresh-cut CR was compared with traditionally processed CR (CR-T), and the optimal moisture content for fresh cutting was established. Quality assessments were conducted using fingerprint analysis and multivariate statistical analysis to identify differential components. Additionally, network pharmacology and molecular docking were employed to predict associated diseases and mechanisms, which were subsequently validated *in vivo* using a dysmenorrhea rat model. The findings indicated that CR-F, when dried to a moisture content of 35.95%–45.52%, exhibited superior appearance. No significant differences were found in powder identification, thin-layer chromatography (TLC), moisture content, ash content, extract yield, or aflatoxin levels when compared to CR-T. Notably, CR-F demonstrated significantly higher concentrations of tetrahydropalmatine. Six differential components—tetrahydropalmatine, dehydrocorydaline, (+)-corydaline, palmatine hydrochloride, coptisine hydrochloride, and columbamine—exhibited strong binding affinities to core targets such as ESR1, STAT3, MMP9, mTOR, and PTSG2, thereby modulating steroid hormone biosynthesis and estrogen signaling pathways. Furthermore, CR-F significantly restored the levels of 5-HT, $PGF_{2\alpha}$, 6-Keto-$PGF_{1\alpha}$, GSH, and MDA in dysmenorrhea-induced rats, demonstrating more potent analgesic effects compared to CR-T. This study underscores the efficacy of fresh-cut processing in preserving tetrahydropalmatine and enhancing the analgesic properties of CR, thereby supporting the establishment of quality standards and facilitating large-scale production of fresh-processed CR.

Keywords: *Corydalis Rhizoma*, Fresh processing, Differential components, Network pharmacology, Dysmenorrhea

Citation: Yang H, Li B, Li Z, Zhao H, Zheng N, et al. 2026. The influence of different processing methods on the quality and pharmacological effects of harvested *Corydalis Rhizoma*. *Medicinal Plant Biology* 5: e019 https://doi.org/10.48130/mpb-0026-0015

Introduction

Corydalis Rhizoma (CR), also known as *Corydalis yanhusuo*, YuanHu, YanHu, or XuanHu in China, is a prominent Traditional Chinese Medicine (TCM) derived from the dried tubers of *Corydalis yanhusuo*[1]. It has been utilized extensively in clinical practice for over 2,000 years[2]. To date, more than 160 compounds have been identified in CR, including alkaloids, steroids, organic acids, amino acids, essential oils, nucleosides, and saccharides[3,4]. Recent medical research has demonstrated that CR possesses significant analgesic, sedative, and hypnotic effects, yielding favorable clinical outcomes in the treatment of conditions such as cardiac arrhythmia, gastric ulcers, and coronary heart disease[2,5]. The distribution of CR spans several regions, including Anhui, Jiangsu, Zhejiang, Hubei, and Hunan, with primary production areas located in Hanzhong in Shaanxi and Pan'an in Zhejiang[6]. Notably, Chenggu County in Shaanxi Province serves as a major cultivation base for *Corydalis yanhusuo*, recognized as a representative 'Qin Medicine'.

For traditional Chinese medicine, achieving maximal yields of bioactive constituents remains a significant challenge, intricately influenced by numerous variables including seeding selection, cultivation techniques, storage conditions, and transportation logistics[7,8]. Therefore, the processing and preparation of traditional Chinese medicine are critical factors influencing the quality of the final medicinal product[9]. The conventional method for processing Chinese medicinal materials typically involves the removal of impurities, followed by washing, drying, and preliminary processing at the site of harvest. Subsequent procedures include soaking, softening, cutting, and further drying[10]. However, the extended duration required for drying and soaking can lead to issues such as mold growth and contamination. Additionally, the infiltration process may result in the dissolution and loss of constituents, as well as hydrolysis and enzymatic degradation, thereby increasing the likelihood of substandard quality in traditional Chinese medicine decoction pieces[11,12]. Thus, optimizing the moisture content during fresh processing is crucial for preserving active metabolites, ensuring quality, and improving processing efficiency[13]. In response to these challenges, the General Office of the State Council of China, in 2015, defined 'fresh cut processing' as 'the technique of processing freshly harvested Chinese medicinal materials by directly cutting or suitably processing them into slices, segments, blocks, petals, etc., followed by drying'. The approach was advocated to promote 'fresh-cut processing and deep processing'[11]. The integrated study of fresh processing and traditional Chinese medicine processing holds practical significance in reducing the production cycle of decoction pieces, enhancing the content ratio of active ingredients, and improving pharmacological activity[14]. Its applicability has been validated in various Chinese medicinal materials, including Curcumae Radix[15], Rhubarb[16], Polygoni Multifloria Radix[17], *Salvia miltiorrhiza* Bunge[18], and *Scutellaria baicalensis* Georgi[19].

https://doi.org/10.48130/mpb-0026-0015

The conventional processing method for CR involves several steps: impurity removal, washing, boiling until the core is no longer white, sun drying, re-washing, moistening, slicing into thick pieces, and a final sun drying, as prescribed by the Chinese Pharmacopoeia[20]. This traditional method includes secondary soaking and softening, which accelerates the loss of water-soluble alkaloid components. Furthermore, the harvested medicinal materials have a high moisture content and, if not processed promptly, are susceptible to mildew and rot, significantly compromising their quality, clinical efficacy, and economic value[21]. Currently, there are no studies available on the effects of fresh processing on the quality and efficacy of CR.

This study systematically investigates the fresh processing of CR, with a particular focus on the influence of moisture content during the cutting process. It examines the effects of both fresh and traditional cutting methods on the microscopic characteristics, thin layer, moisture content, ash content, ethanol-soluble extract, tetrahydropalmatine content, and overall appearance of CR. Using fingerprint spectra and multivariate statistical analysis, we identified differential components between CR-F and CR-T. Furthermore, the analgesic effects of CR-F and CR-T were assessed through network pharmacology, molecular docking, and dysmenorrhea rat models. This study not only provides a foundation for post-harvest processing in CR producing regions, but also offers data support for the development of technical specifications and quality standards for fresh cutting and processing in these areas.

Materials and methods

Materials and reagents

The fresh CR was purchased from Chenggu County, Hanzhong City, Shaanxi Province, and identified by Dr. Hong Zhang from the Shaanxi Academy of Traditional Chinese Medicine as tubers of *Corydalis yanhusuo* W.T. Wang, a plant in the Papaveraceae family. The reference medicinal materials of *Corydalis Rhizoma* and the reference substances of tetrahydropalmatine and berberine hydrochloride were supplied by the National Institutes for Food and Drug Control. The reference substance of protopine, coptisine hydrochloride, dehydrocorydaline, dihydrosanguinarine, (R)-(+)-corypalmine, (+)-corydaline, columbamine, and palmatine hydrochloride were obtained from Chengdu Chroma-Biotechnology Co., Ltd. Estradiol benzoate injection was purchased from Shanghai Quanyu Biotechnology Co., Ltd. Oxytocin injection was from Shanghai Harvest Pharmaceutical Co., Ltd. Tongjingbao granules were procured from Nanjing Zhangda Tianqing Pharmaceutical Co., Ltd. 5-HT, β-EP, TXB_2, 6-Keto-$PGF_{1\alpha}$, PGE_2, and $PGF_{2\alpha}$ assay kits were provided by Wuhan Feien Biotechnology Co., Ltd. MDA, CAT, SOD, and GSH assay kits were supplied by Nanjing Jiancheng Bioengineering Institute. The BCA protein assay kit was obtained from Shanghai Biyuntian Biotechnology Co., Ltd.

Animals

Female Sprague–Dawley (SD) rats (180–220 g) were procured from the Chengdu Dashuo Animal Experiment Center, holding the license number SCXK (Chuan) 2020-030. The rats were maintained in a controlled environment with a temperature range of 20–25 °C, relative humidity of 40%–60%, and a 12-h light/dark cycle. They were provided with a standard rodent diet and water *ad libitum*. The Ethical Committee of Shaanxi Academy of Traditional Chinese Medicine (NWU-AWC-20240601M) approved the study.

The fresh cutting process of CR

Pre-treatment of fresh medicinal herbs of CR

Initially, the fresh medicinal material of CR underwent an impurity removal process to eliminate non-medicinal components. The purified herbs were then transferred to a clean area and subjected to thorough rinsing with a continuous water flow until no sediment remained on their surfaces. Following this cleaning process, the fresh CR was boiled until the white core was no longer present. The boiled material was subsequently laid flat on a drying plate to air dry naturally and was then labeled accordingly.

Preparation of fresh cut medicinal herbs from CR

A total of nine batches of fresh CR were collected from Shangyuanguan Town, Shaheying Town, and Sanhe Town in Chenggu County, Shaanxi Province. These batches were subjected to the aforementioned pre-treatment process. Afterwards, once the surface moisture of the CR evaporated, sampling was conducted in accordance with General Rule 0212 of the Chinese Pharmacopoeia 2020 edition[20]. The freshly obtained CR was then sliced into thick sections (2–4 mm) and immediately dried. The moisture content is periodically assessed until the slices can no longer be cut. Ultimately, fresh-cut samples of CR that exhibit characteristics similar to those of traditionally processed pieces are selected for each batch. This selection is based on a comparative analysis of the color of the cut surface, the presence of curled and fragmented pieces, and the occurrence of slag and fragments, as per traditional processing methods. The moisture content and appropriate cutting moisture range for the nine batches of freshly cut CR are then calculated.

Quality assessment of CR-F

The powder identification, thin-layer chromatography identification, moisture content, total ash content, extract yield, and the content of tetrahydropalmatine in fresh-cut CR were determined according to the Chinese Pharmacopoeia 2020 edition[20].

Comparative quality analysis between fresh cutting and traditional processing of CR

Preparation and quality assessment of fresh-cut and traditional-processed CR pieces

Three batches of fresh medicinal materials of CR were collected from Liangjia'an Village, Chenggu County. From each batch, a portion of the medicinal materials was selected and sliced into fresh CR slices following the fresh-cut process, while another portion underwent traditional processing to produce CR slices. After impurities were removed and the remaining 50% of fresh CR medicinal materials from each batch were washed, they were boiled until the white core was no longer present and subsequently dried to obtain the CR dried medicinal materials. These dried medicinal herbs were then thoroughly washed, cut into thick slices, and dried to achieve the traditional processing of CR. Subsequently, the indicators specified in Section 2.3.3 of the Chinese Pharmacopoeia 2020 edition were assessed.

Establishment of a comprehensive scoring system

A comprehensive scoring standard for CR fresh slices and traditionally processed slices was established, taking into account appearance, molding rate, ethanol-soluble extract, and content of tetrahydropalmatine, with respective weight coefficients of 0.2, 0.1, 0.3, and 0.4[22]. The criteria for evaluating appearance traits are shown in Supplementary Table S1, and the calculation formula is as follows:

$Y = 0.2 \times (S_{1i} - S_{1min})/(S_{1max} - S_{1min}) + 0.1 \times (S_{2i} - S_{2min})/(S_{2max} - S_{2min}) + 0.3 \times (S_{3i} - S_{3min})/(S_{3max} - S_{3min}) + 0.4 \times (S_{4i} - S_{4min})/(S_{4max} - S_{4min})$

where i represents the group number, S_{1i}, S_{2i}, S_{3i}, and S_{4i} refer to the appearance score, molding rate score, alcohol soluble extract, and tetrahydropalmatine content of each group, respectively. S_{1max}, S_{2max}, S_{3max}, S_{4max}, and S_{1min}, S_{2min}, S_{3min}, and S_{4min} correspond to the maximum and minimum values of all group appearance scores, molding rate scores, alcohol soluble extract, and tetrahydropalmatine content, respectively.

Establishment of fingerprint spectrum

LC conditions

Chromatographic separation was conducted using an Agilent ZORBAX C_{18} column (4.6 mm × 250 mm, 5 μm) under a gradient of 0.1% aqueous phosphoric acid in water (A) and acetonitrile (B), utilizing an Agilent 1260 System. The gradient elution was programmed as follows: 10%–17% B (0–15 min), 17%–25% B (15–65 min), 25%–55% B (65–85 min), 55%–80% B (85–105 min), 80%–85% B (105–115 min), 85%–10% B (115–130 min), with a flow rate of 1.0 mL·min^{-1} and an injection volume of 10 μL. The detection wavelength was set at 280 nm.

Validation of methodology

The sample solution of CR-F was accurately prepared in accordance with the sample preparation protocol delineated in the 2020 edition of the Chinese Pharmacopoeia for quantifying the content of tetrahydropalmatine. Subsequently, the sample underwent six injections adhering to the chromatographic conditions in section "LC conditions" to assess precision. The stability of the CR-F solution was evaluated at intervals of 0, 4, 6, 8, and 12 h. Following this, six replicates of the CR-F solution were injected to examine the reproducibility of the CR solution.

Establishment and evaluation of the fingerprint

Twenty batches of fresh-cut CR and traditionally processed pieces were prepared as test solutions. Chromatograms were recorded via LC detection, and the data were imported into the 'Chinese Medicine Chromatographic Fingerprint Similarity Evaluation System' (2012 version) to establish characteristic peak fingerprint spectra for the two processing methods of CR.

Analysis of differential components

The peak areas of 24 common peaks in the fingerprint spectra of the 20 batches of CR-F and CR-T were imported into SMICA software for HCA and OPLS-DA analysis to identify differential components. The peak areas of the six differential characteristic peaks were log-normalized for heatmap analysis to elucidate the variations in chemical composition between CR-F and CR-T.

Mechanism of pharmacological effects of CR-F and CR-T

Network pharmacology

The Swiss Target Prediction database was utilized to predict targets for six differential components. The identified targets were then imported into the STRING database with a high confidence threshold set at 0.4 to generate a TSV format file, which was subsequently imported into Cytoscape 3.7.2. A protein–protein interaction (PPI) network graph was constructed by screening the top 30 core targets based on degree values. Cytoscape 3.7.2 was further employed to create a 'differential component-core target' graph, from which the top 10 core targets were selected based on degree values. These core targets were then subjected to GO and KEGG biological enrichment analysis using the DAVID database, followed by visualization analysis.

Molecular docking

The molecular structures of dehydrocorydaline, tetrahydropalmatine, palmatine hydrochloride, columbamine, coptisine hydrochloride, and (+)-corydaline were generated from canonical simplified molecular-input line-entry system (SMILES) strings retrieved from the PubChem database. The lowest-energy conformations were generated using the MM2 force field in ChemBio3D Ultra 12.0 and subsequently saved in the mol2 file format. Concurrently, the 3D crystal structures of ERS1 and PTGS2 were retrieved from the Protein Data Bank and processed using AutoDockTools-1.5.6 to add hydrogen atoms and remove water molecules. Molecular docking was executed by inputting instructions into Vina. The results were then visualized using PyMOL software.

Pharmacodynamic studies

Extraction of CR-F and CR-T

A total of 60 g of CR-F and CR-T were subjected to boiling 3 times with 10 times the volume of water, each for a duration of 90 min. The resulting filtrate was combined and concentrated to yield water extracts of CR-F and CR-T with concentrations of 0.126 and 0.141 g·mL^{-1}, respectively.

Establishment of the dysmenorrhea model and drug treatment

Fifty-six female rats were randomly assigned to one of seven groups: control group, model group, low-dose CR-F (0.45 g·kg^{-1}), high-dose CR-F (1.8 g·kg^{-1}), low-dose CR-T (0.45 g·kg^{-1}), high-dose CR-T (1.8 g·kg^{-1}), and positive (2.1 g·kg^{-1} Tongjingbao granules). All experimental groups, with the exception of the control group, received intraperitoneal injections of estradiol benzoate for a duration of 10 consecutive days. The dosage administered was 2.5 mg·kg·d^{-1} from days 1 to 10, and 1.25 mg·kg·d^{-1} from days 2 to 9. Following the final administration, each group of rats was intraperitoneally injected with five units of oxytocin 1 h post-dosing. The pain response of the rats was monitored for 30 min, during which the frequency of writhing and the latency to writhing were recorded. Commencing on the 11th day, each treatment group received oral administration of varying concentrations of CR-F and CR-T, as well as Tongjinbao granules, for a period of 7 consecutive days. Following the final administration, the animals were subjected to a 12-h fasting period without water. Blood samples were collected from the abdominal aorta and centrifuged at 3,500 r·min^{-1} for 15 min at 4 °C to separate the serum, which was subsequently aliquoted and stored at −80 °C. Meanwhile, uterine tissues from each group were collected and stored at −80 °C for further analysis.

Detection of the biochemical indicators

The levels of 5-HT and β-EP in the serum, as well as the concentrations of 6-Keto-PGF$_{1\alpha}$, TXB_2, PGE_2, PGF$_{2\alpha}$, SOD, CAT, GSH, and MDA in uterine tissues, were measured according to the manufacturer's instructions of the ELISA kits.

Pathological observation of the uterus

Following fixation of the uterine tissues from each group of rats using 4% paraformaldehyde, histopathological alterations were examined through H&E staining.

Data analysis

Statistical analysis of the data was conducted using SPSS 23.0, with results expressed as the mean ± SD. Inter-group differences were assessed via an unpaired t-test, with statistical significance determined at $p < 0.05$.

https://doi.org/10.48130/mpb-0026-0015

Results

The moisture content range of CR-F

The variation in moisture content of CR-F is depicted in Fig. 1a, indicating a continuous decrease in moisture content with increased drying time of CR. By the eighth cut, the moisture content of CR-F approaches 20%. A comparative analysis of the medicinal properties and moisture content of nine batches of CR-F, each subjected to eight cuts, was conducted against CR-T, which was cut using traditional methods, to identify samples with similarities to both CR-F and CR-T. Figure 1b illustrates that the optimal moisture content range for cutting CR is between 29.45% and 47.72%. Moisture content exceeding 47.72% results in uneven surfaces, curling, and edge rolling post-cutting, while moisture content below 29.45% renders CR difficult to cut, leading to rough cut surfaces with fragments and medicinal residues. This analysis is based on the upper and lower quartiles; the suitable moisture range for cutting nine batches of CR is 35.95%–44.52%.

Quality comparison between CR-F and CR-T pieces

The results of the powder microscopic identification of CR-F and CR-T are shown in Fig. 2a, where threaded conduits, colorless gelatinized starch granules, and yellow-green thick-walled cells of various shapes are observable. In the TLC chromatogram analysis, fluorescent spots corresponding to the reference standard of THP and reference material of CR were observed in the chromatograms of CR-T and CR-F, aligning both in position and color (Fig. 2b). The moisture, ash content, and extractive content of various batches of CR-F and CR-T were measured, as depicted in Fig. 2c–e. The moisture content ranged from 7.96% to 8.13% (≤ 15%), the total ash content ranged from 2.15% to 2.50% (≤ 4.0%), and the extractive content ranged from 13.07% to 13.14% (≥ 13%). These values are in compliance with the standards set by the Chinese Pharmacopoeia (version 2020)[20], and no significant differences were observed between CR-F and CR-T in these parameters. The THP content is presented in Fig. 2f, with CR-F batches exhibiting a THP content range of 0.1038% to 0.1082%, which is significantly higher than that of CR-T, ranging from 0.0964% to 0.09875%. The results are illustrated in Fig. 2f. Furthermore, the analysis of aflatoxin content revealed that no aflatoxins were detected in either CR-F or CR-T (Fig. 2g). Furthermore, the appearance traits of CR-F and CR-T were evaluated with scores of 4.9 and 3.7, respectively. When these scores were integrated with their molding rate, ethanol-soluble extract, and the THP content, the comprehensives were calculated as 0.6 and 0.1, respectively, indicating a significantly higher comprehensive score for CR-F compared to CR-T (Fig. 2h, i).

Fingerprint spectrum

Peak 12, identified as tetrahydropalmatine, was selected as the reference peak for assessing the HPLC fingerprinting methodology due to its excellent stability and appropriate peak area. Additionally, the relative standard deviations (RSDs) for the relative retention times and relative peak areas of the other 23 peaks were below 3%, demonstrating the method's superior precision, stability, and repeatability, thereby confirming its suitability for CR fingerprinting. The HPLC chromatograms of 20 batches of CR-F and CR-T were analyzed using the 'Similarity Evaluation System for the Chromatographic Fingerprint of TCMs' (version 2012), resulting in the establishment of characteristic peak fingerprint spectra for the two CR processing methods, as depicted in Fig. 3a and b. Twenty-four common peaks were selected based on consistent retention time, satisfactory separation, and peak shape, with their relative peak areas detailed in Supplementary Tables S2 and S3. Through comparison with reference substances, 10 common peaks were identified, including columbamine (peak 5), (R)-(+)-corypalmine (peak 7), protopine (peak 10), tetrahydropalmatine (peak 12), coptisine hydrochloride (peak 14), (+)-corydaline (peak 15), palmatine hydrochloride (peak 18), berber inehydrochloride (peak 19), dehydrocorydaline (peak 20), and dihydrosanguinarine (peak 24). The similarity indices for 20 batches of CR-F and CR-T ranged from 0.900 to 0.998 and 0.975 to 0.998, respectively (Supplementary Table S4), suggesting compositional differences between the samples and indicating a relatively stable sample quality, thereby confirming the stability of the fresh cutting process.

Differential component screening between CR-F and CR-T

The hierarchical cluster analysis (HCA) results are shown in Fig. 4a, showing that the 20 batches of CR-F form one distinct cluster, while the 20 batches of CR-T form another, highlighting compositional differences between CR-F and CR-T. Utilizing SMICA for OPLS-DA analysis, the findings are presented in Fig. 4b, demonstrating that CR-F and CR-T can be categorized, aligning with the outcomes of HCA. This further suggests the presence of distinctions between CR-F and CR-T. Additionally, the components contributing to the differences between CR-F and CR-T were identified using a variable importance projection (VIP) value ≥ 1 as the selection criterion. Consequently, tetrahydropalmatine, dehydrocorydaline, (+)-corydaline, palmatine hydrochloride, coptisine hydrochloride, and columbamine were identified as the primary differential components between CR-F and CR-T (Fig. 4c, d). Subsequently, heatmap analysis was conducted on the HPLC characteristic spectra data of CR-F and CR-T employing the peak area of six differential characteristic peaks as variables. The analysis revealed a significant difference in the chemical composition between CR-F and CR-T (Fig. 4e).

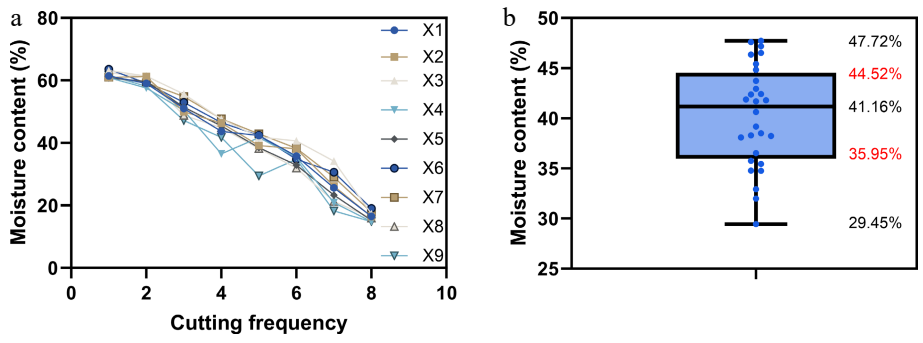

Fig. 1 (a) Trend of moisture content change, and (b) the moisture content range of CR-F.

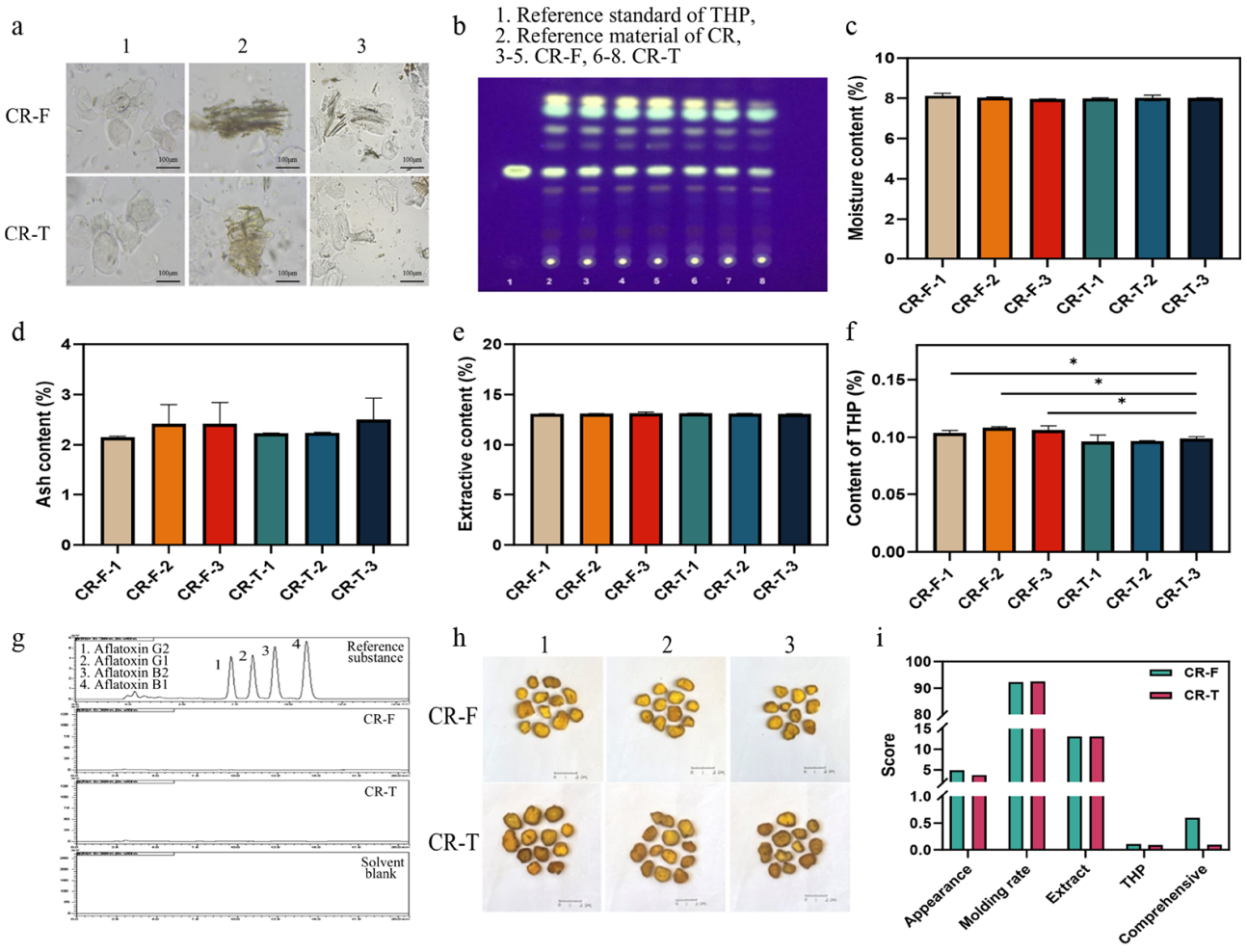

Fig. 2 The effect of fresh cutting and traditional processing on the quality of CR. (a) Microscopic identification characteristics of powder. (b) Thin layer chromatogram. (c) Moisture content. (d) Ash content. (e) Extractive content. (f) THP content. (g) HPLC chromatogram of aflatoxin. (h) Appearance characteristics. (i) Comprehensive score. Data are expressed as the mean ± SD (n = 3).

Network pharmacology analysis

The Swiss Target Prediction database was then utilized to predict the targets of six differential components, resulting in the identification of 268 targets. These targets were subsequently imported into the STRING database, applying a high confidence threshold of 0.4 as the screening criterion. The obtained key targets were imported into Cytoscape 3.7.2 in TSV format, resulting in the construction of a core target diagram using targets with a degree greater than 30, as depicted in Fig. 5a. Subsequently, the six differential components were linked to the core targets to generate a network diagram of 'differential component-targets', as shown in Fig. 5b. The top 10 targets identified were ESR1, STAT3, MMP9, MTOR, PTGS2, CYP19A1, NOS3, MMP2, AKT2, and ADRB2. Furthermore, gene ontology (GO) analysis of the core targets revealed associations with biological processes such as single-organism metabolic processes and cellular responses to stress. Regarding cellular components, these targets are associated with the plasma membrane, endosome, and endoplasmic reticulum membrane, among others. In terms of molecular function, they are related to heme binding and oxidoreductase activity, as shown in Fig. 5c. Additionally, KEGG pathway enrichment analysis indicated that these core targets are implicated in pathways related to endocrine resistance, steroid hormone biosynthesis, and the estrogen signaling pathway, as presented in Fig. 5d.

Molecular docking analysis

Molecular docking analyses were conducted to assess the interactions between six differential components and the core targets (ERS1, STAT3, MMP9, mTOR, and PTGS2) as shown in Fig. 6 and Supplementary Table S5. It is widely recognized that a binding energy of below −5 kcal/mol suggests a potential for ligand and receptor complex formation. The predicted binding energies for all interactions between the six compounds and each of the five proteins were < −5 kcal/mol, suggesting strong binding affinities of these compounds to the five target proteins (Supplementary Table S5).

Pharmacodynamic studies

The effects of CR-F and CR-T on body weight, twisting frequency, and twisting latency in dysmenorrhea rats

Following the establishment of a dysmenorrhea model, the body weight of the rats was measured. On the 10th day, the body weight of the model group was significantly lower than that of the control group ($p < 0.05$). Treatment of dysmenorrhea rats with CR-T and CR-F mitigated the weight loss ($p < 0.05$), but there is no significant effect between CR-T and CR-F, indicating that the processing method does not influence the efficacy of CR in reducing the weight loss trend of dysmenorrhea rats (Fig. 7a). In addition, the model

https://doi.org/10.48130/mpb-0026-0015

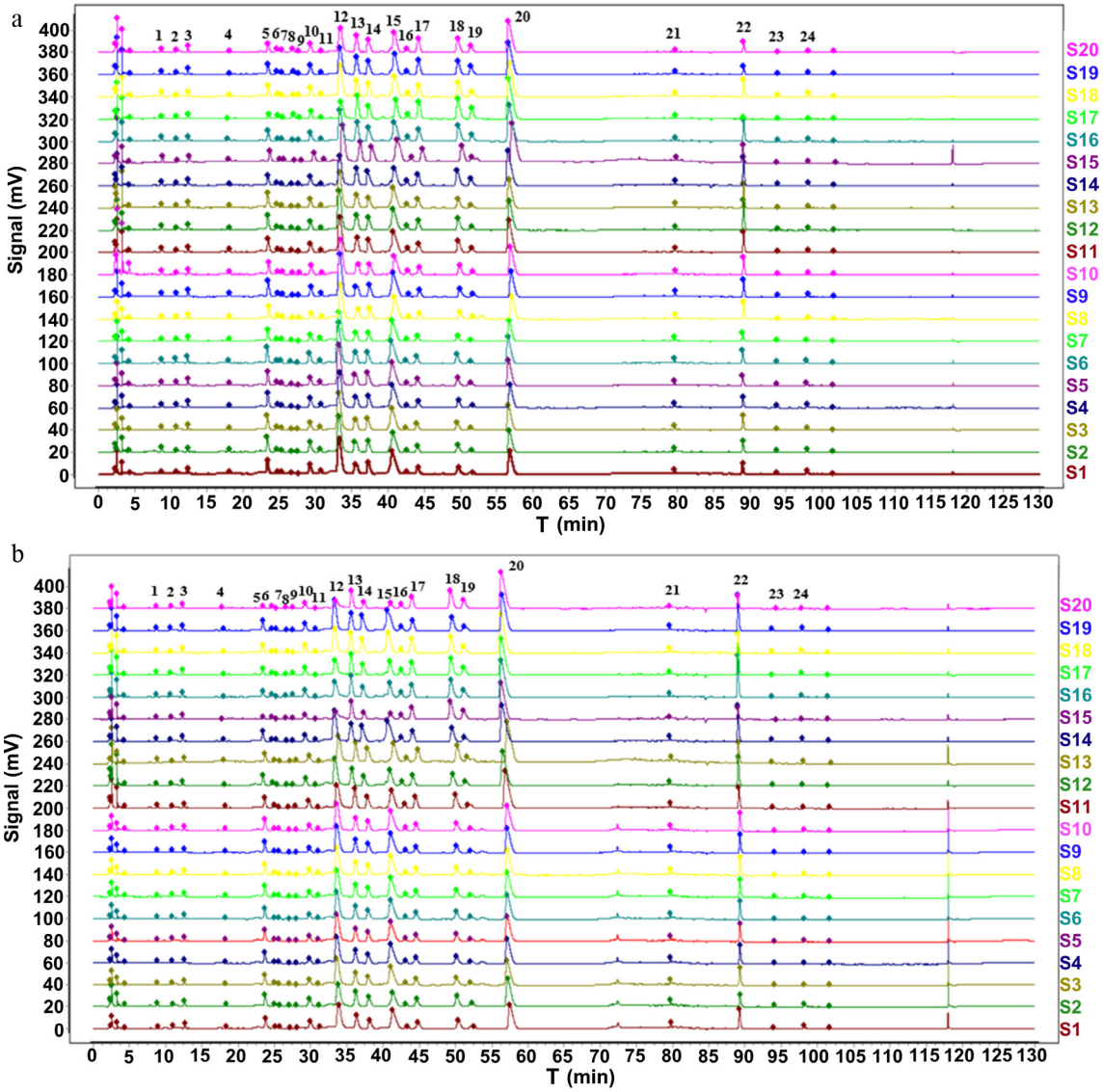

Fig. 3 Fingerprint spectrum of 20 batches of (a) CR-F and (b) CR-T pieces.

group exhibited a significant increase in both the frequency of twisting and the latent period of twisting compared to the control group ($p < 0.01$) (Fig. 7b, c). In comparison to the model group, both CR-F and CR-T significantly decreased the frequency of twisting and extended the latency period ($p < 0.05$), but no significant difference was observed between CR-F and CR-T (Fig. 7b, c).

The effects of CR-F and CR-T on uterine pathological changes in dysmenorrhea rats

The pathological analysis of uterine tissues across the different rat groups is presented in Fig. 7d. The control group exhibited a regular columnar mucosal epithelial structure in the endometria, whereas the model group displayed notably dilated glandular cavities, significant endometrial edema, and extensive vacuolar degeneration and apoptosis in epithelial cells. These findings confirm the successful establishment of the primary dysmenorrhea rat model. Treatment with the positive drug, CR-F, and CR-T, resulted in reduced inflammatory infiltration and the near-complete elimination of eosinophilic mass in the uterine glandular cavity, indicating that CR-F and CR-T ameliorate the uterine pathology associated with dysmenorrhea in rats.

The effects of CR-F and CR-T on the secretion of 5-HT and β-EP in the serum of dysmenorrhea rats

The serum levels of 5-HT and β-EP of each rat group are shown in Fig. 7e and f. The findings demonstrated a significant increase in the content of 5-HT in the serum of the model group rats, reaching 65.33 ± 7.53 ng/mL compared to the control group ($p < 0.01$). Conversely, the content of β-EP was significantly reduced to 448.68 ± 32.37 pg/mL ($p < 0.01$), confirming the successful establishment of the dysmenorrhea rat model. Following treatment with CR-F and CR-T, the serum levels of 5-HT and β-EP in the treated groups exhibited varying degrees of recovery relative to the model group. Notably, CR-F demonstrated a more pronounced effect in ameliorating serum 5-HT levels in dysmenorrhea rats compared to CR-T ($p < 0.05$).

The effects of CR-F and CR-T on the prostaglandin and oxidative stress levels in the uterus of dysmenorrhea rats

The impact of CR-F and CR-T on prostaglandin-related indicators in the uteri of dysmenorrhea rats is shown in Fig. 8a–d. The findings indicate that the levels of $PGF_{2\alpha}$ and TXB2 in the model group were significantly elevated to 131.51 ± 2.09 pg/mL and 218.96 ± 2.48

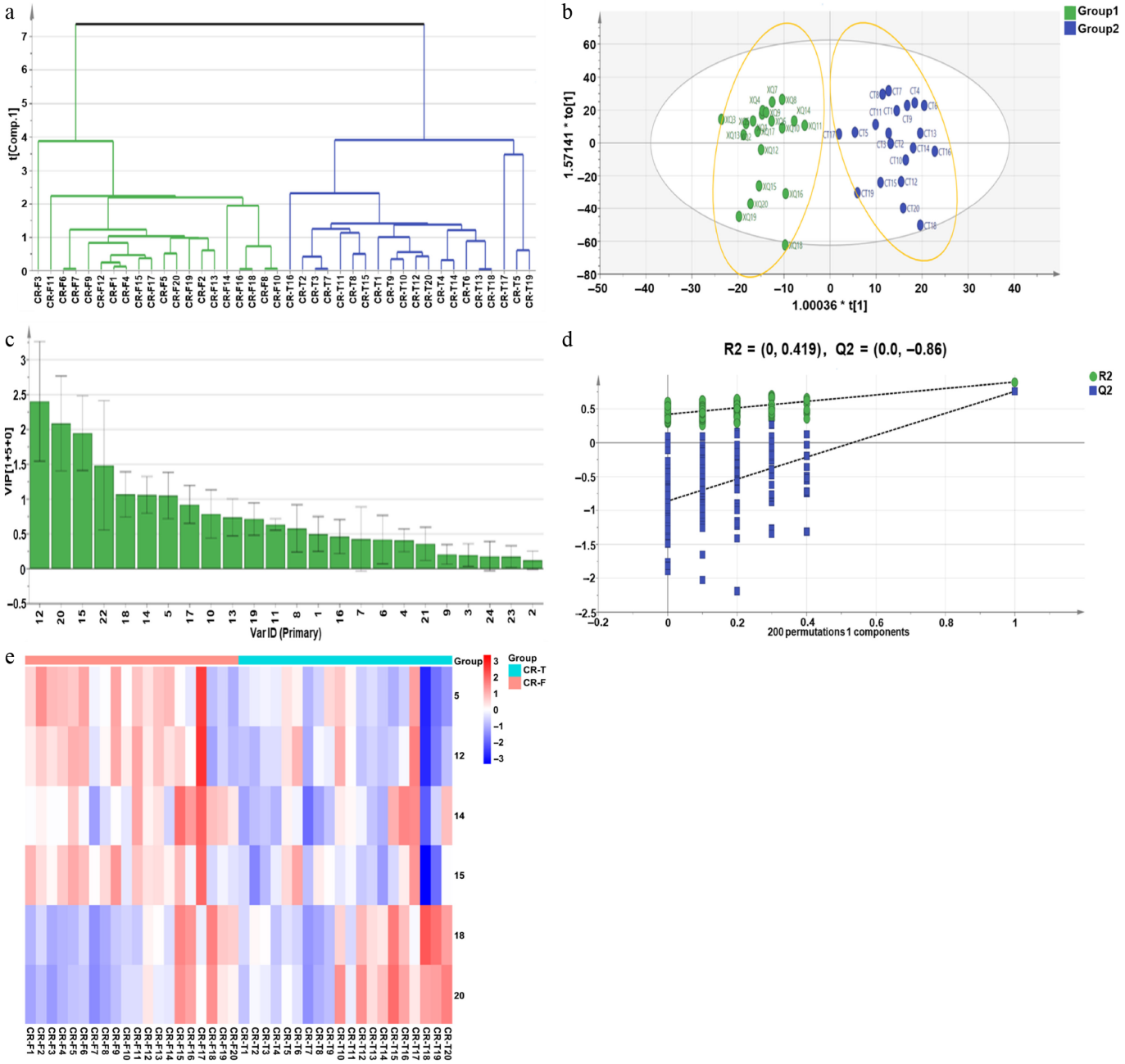

Fig. 4 Differential component analysis of CR-F and CR-T. (a) HCA. (b) OPLS-DA score chart. (c) VIP distribution map of the OPLS-DA model. (d) Permutation detection of the OPLS-DA model. (e) Heatmap analysis.

pg/mL, respectively ($p < 0.01$), when compared to the control group. Conversely, the concentrations of PGE2 and 6-Keto-$PGF_{1\alpha}$ were significantly diminished to 13.24 ± 1.22 pg/mL and 577.06 ± 9.99 pg/mL, respectively ($p < 0.001$). In comparison to the model group, the levels of $PGF_{2\alpha}$ and TXB2 in the uteri of rats subjected to each pharmacological treatment were significantly reduced, whereas the levels of PGE2 and 6-Keto-$PGF_{1\alpha}$ were significantly elevated ($p < 0.05$). Notably, CR-F exhibited a more pronounced ameliorative effect on $PGF_{2\alpha}$ and 6-Keto-$PGF_{1\alpha}$ than CR-T ($p < 0.05$). Analysis of oxidative stress indicators revealed that the activities of SOD, CAT, and GSH in the model group were significantly decreased to 40.84 ± 0.31, 64.81 ± 13.00, and 156.74 ± 7.09 μmol/mgprot, respectively ($p < 0.01$) (Fig. 8e, f, h). Additionally, the MDA content was significantly increased to 1.608 ± 0.218 nmol/mgprot ($p < 0.01$) (Fig. 8g). These results suggest that dysmenorrhea can induce oxidative stress in rats. Following treatment with CR-F and CR-T, the levels of SOD, CAT, GSH, and MDA in the uterine tissue of all rat groups demonstrated a tendency to return to normal levels. Notably, CR-F exhibited a significantly superior capacity to enhance GSH and MDA levels compared to CR-T ($p < 0.05$).

Discussion

Moisture content is a critical determinant of the characteristics and quality of freshly cut medicinal herbs. Excessive moisture can complicate the cutting process, leading to uneven cuts and adversely affecting both the appearance and internal quality of the

https://doi.org/10.48130/mpb-0026-0015

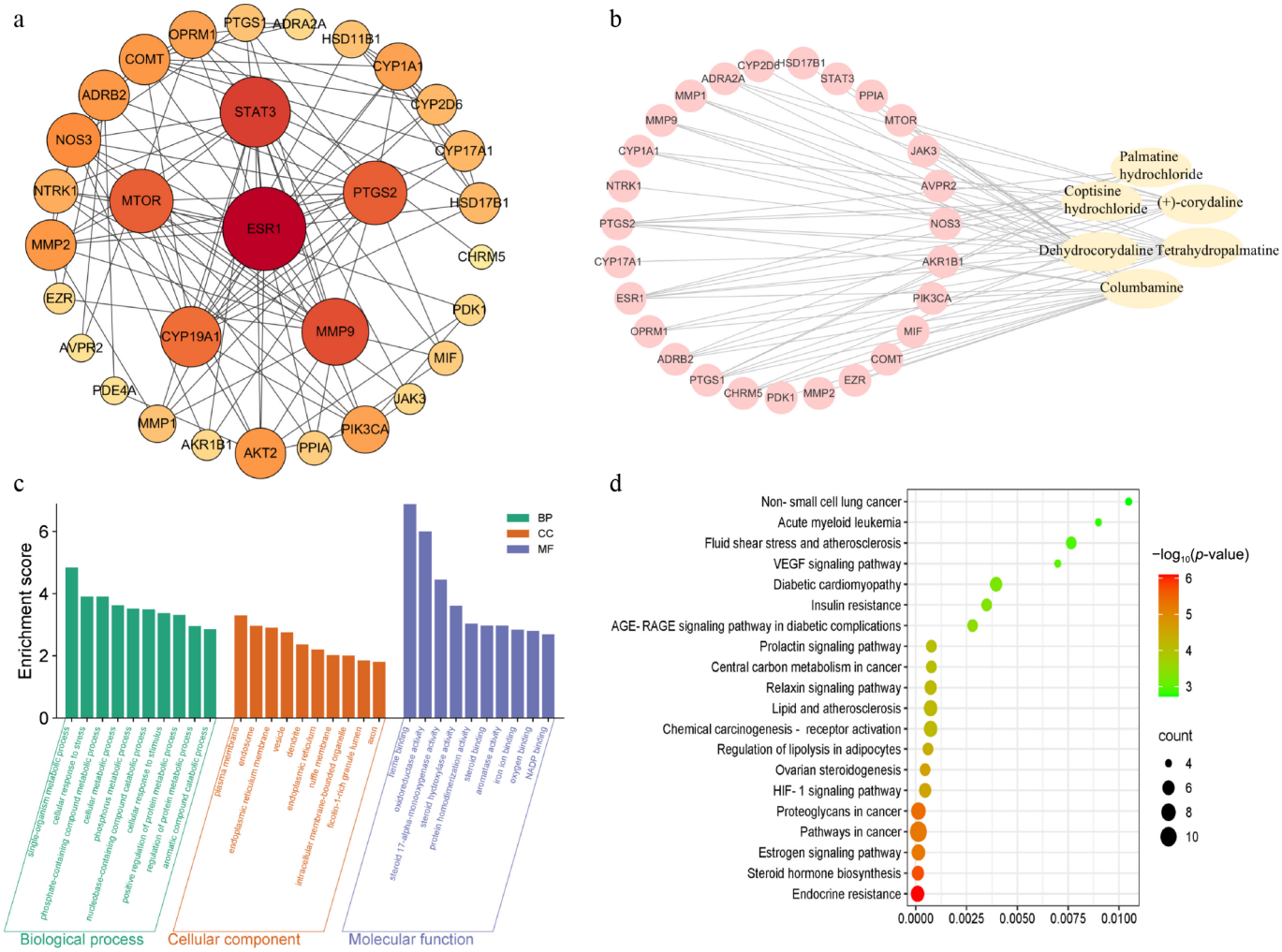

Fig. 5 Network pharmacology analysis of differential components between CR-F and CR-T. (a) PPI network of differential components targets. (b) Network diagram of 'differential components-core targets'. (c) GO analysis of core targets. (d) KEGG pathway enrichment analysis of core targets.

herbs. Moreover, controlling the moisture content is currently the most prevalent and effective strategy for inhibiting mold growth[23]. Consequently, we conducted a systematic investigation to determine the optimal moisture content range for the fresh cutting of CR to ensure its desirable appearance characteristics. Given the hard and dense texture of CR, traditional processing methods necessitate prolonged soaking, and uneven water infiltration can result in the undesirable condition of being 'soft outside and hard inside'. Fragmentation can readily occur during cutting, and excessive infiltration may result in a substantial loss of active constituents, thereby compromising the quality of the decoction pieces. Furthermore, during the fresh cutting process, it has been observed that high moisture content can lead to uneven cutting surfaces, as well as warping and curling of edges. Conversely, low moisture content poses challenges in cutting, resulting in rough surfaces with numerous fragments and lobes. Research indicates that the optimal moisture content for fresh processing of licorice and *Angelica dahurica* is 50%[24,25]. A reduction in the moisture content of licorice is associated with a continuous increase in the b* value of its sliced slices, which significantly affects their color[24].

Studies have demonstrated that fresh-cut Chinese medicinal materials exhibit superior levels of various indicators, such as polysaccharides, flavonoids, saponins, and extracts, compared to traditional cutting methods[26]. Additionally, the content of THP in CR-F is significantly higher than in CR-T, potentially due to fresh processing's ability to prevent secondary infiltration and minimize the loss of chemical components[27]. Wang et al. demonstrated that the fresh cutting process of *Aconiti Lateralis Radix* significantly mitigates the loss of alkaloids[27]. Furthermore, research indicates that the levels of total polysaccharides, total flavonoids, and the active ingredient flavone-7-O-glucoside are markedly higher in freshly processed *Astragali Radix* compared to those subjected to traditional processing methods[28]. The microscopic characteristics, TLC analysis, total ash content, ethanol-soluble extract, and aflatoxin levels of CR-F all meet the requirements of the pharmacopoeia, showing no significant difference when compared to CR-T. Consequently, CR-F not only satisfies pharmacopoeia requirements, but also effectively preserves THP, thereby enhancing the quality of medicinal materials. Additionally, investigations into the fresh cutting process of various traditional Chinese medicinal materials suggest that it maintains superior appearance, potentially by reducing enzymatic hydrolysis reactions prior to drying and safeguarding the stability of thermosensitive components[26], as evidenced by the brighter color of Taraxaci Herba post-fresh cutting[29].

The variation in ingredient composition is a critical factor influencing the efficacy of pharmaceuticals. Subsequent differential

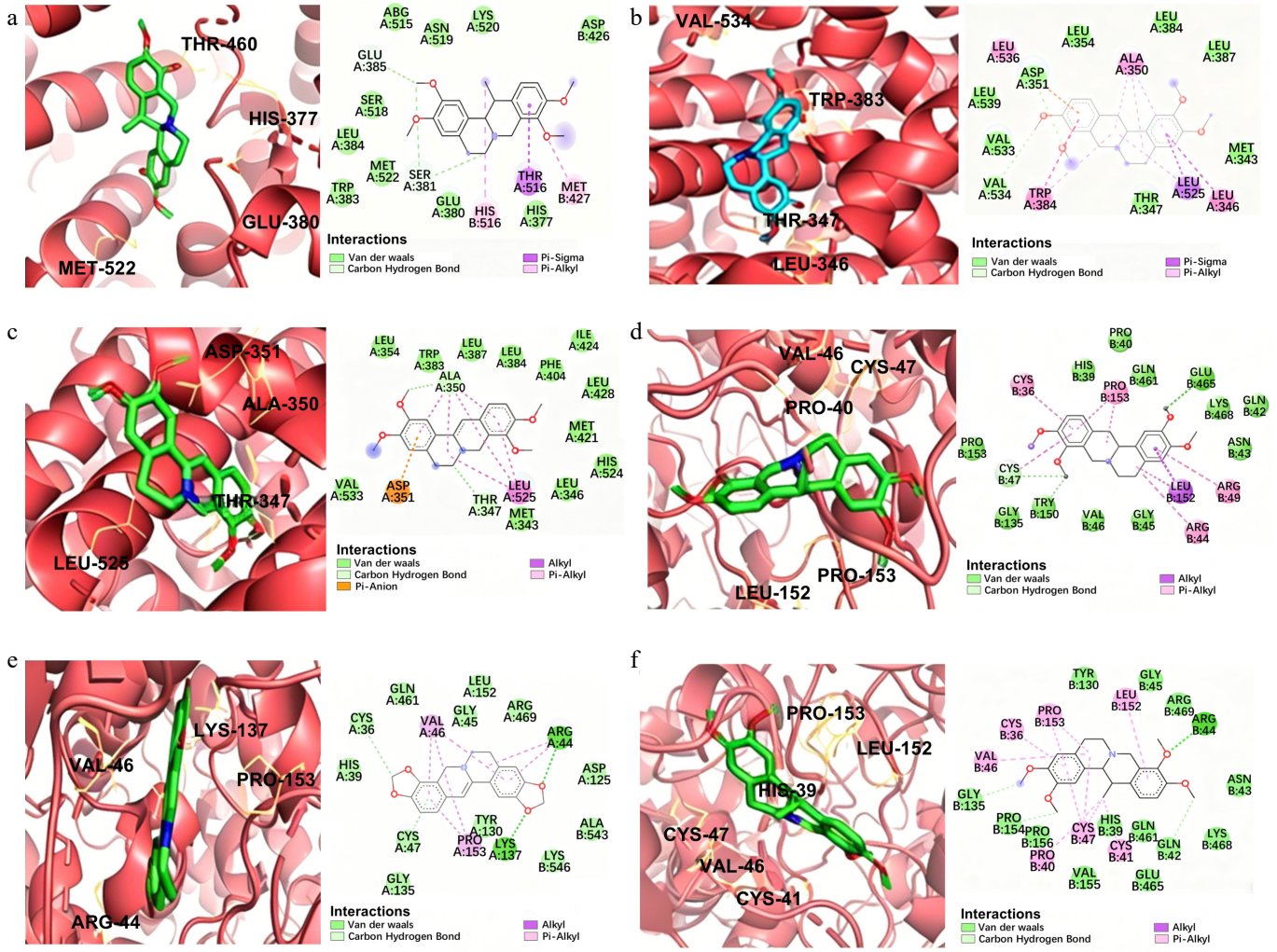

Fig. 6 Molecular docking of active ingredients with key target molecules. (a) 3D and 2D conformation of dehydrocorydaline and ESR1. (b) 3D and 2D conformation of tetrahydropalmatine and ERS1. (c) 3D and 2D conformation of palmatine hydrochloride and ERS1. (d) 3D and 2D conformation of columbamine and PTGS2. (e) 3D and 2D conformation of coptisine hydrochloride and PTGS2. (f) 3D and 2D conformation of (+)-corydaline and PTGS2.

component analysis was performed to examine the variations in peak areas between CR-F and CR-T. This analysis identified tetrahydropalmatine, dehydrocorydaline, (+)-corydaline, palmatine hydrochloride, coptisine hydrochloride, and columbamine as the distinct components differentiating CR-F from CR-T. These compounds are implicated in the estrogen signaling pathway and steroid hormone biosynthesis through their interactions with ESR1, STAT3, MMP9, mTOR, and PTGS2. To further assess the comparative effects of CR-F and CR-T on pharmacological efficacy, a dysmenorrhea model was established. The findings indicated that both processing methods ameliorated dysmenorrhea in rats, and CR-F demonstrated a more significant effect on 5-HT levels in rat serum, as well as on $PGF_{2\alpha}$, 6-Keto-$PGF_{1\alpha}$, GSH, and MDA in the uterus, compared to CR-T. This observation aligns with numerous studies suggesting that the pharmacological activity of freshly cut slices surpasses that of traditionally processed slices. For instance, the integrated processing of medicinal herbs from the production area of Moslae Herba has been shown to be slightly superior to traditional processing methods in terms of antipyretic and anti-inflammatory effects[30], and the total flavonoid content in freshly cut *Astragali Radix* exhibits a more pronounced effect on the activation of macrophage RAW264.7 cells compared to traditionally cut samples[28]. Additionally, its antioxidant activity surpasses that of conventionally cut slices[31].

It is important to highlight that core targets, including ESR1, STAT3, MMP9, mTOR, and PTGS2, were identified through network pharmacology and molecular docking analyses, demonstrating significant topological importance and strong binding affinities to the six differential components. Notably, ESR1 serves as a pivotal receptor in estrogen signaling and the regulation of ovarian function, closely associated with the occurrence and progression of primary dysmenorrhea[32,33]. PTGS2, also known as COX-2, functions as the rate-limiting enzyme in prostaglandin synthesis, directly influencing the production of $PGF_{2\alpha}$, PGE2, and other inflammatory mediators that govern uterine contraction and pain response[33]. Furthermore, contemporary medical understanding largely attributes the pathogenesis of dysmenorrhea to the synthesis and release of prostaglandins, which elicit inflammatory responses contributing to the condition. $PGF_{2\alpha}$ and PGE2 play critical roles in the occurrence and development of dysmenorrhea[34]. Research has demonstrated that $PGF_{2\alpha}$ and PGE2 interact with COX enzymes, leading to increased uterine tension and spasmodic contractions, which subsequently cause uterine ischemia and hypoxia, thereby contributing to the onset of dysmenorrhea[34]. Furthermore, by modulating the expression of PTGS2, the oxidative stress pathway can be influenced to produce antioxidant effects and protect the uterus. The selection of these targets was informed by their pivotal

https://doi.org/10.48130/mpb-0026-0015

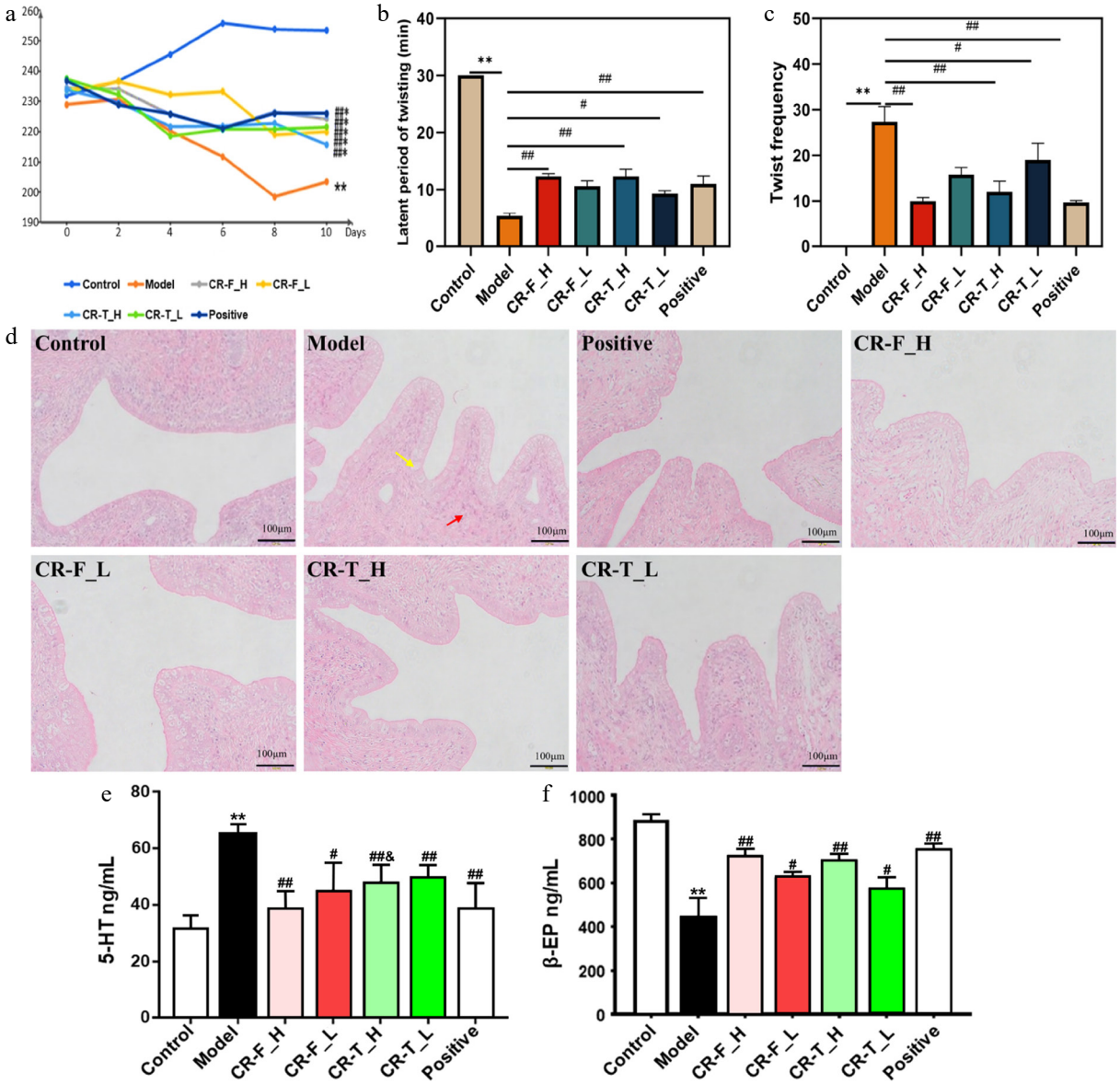

Fig. 7 The effects of CR-F and CR-T on (a) body weight, (b) latent period of twisting, (c) twist frequency, (d) pathological sections of the uterus, (e) 5-HT, and (f) β-EP in the serum of dysmenorrhea rats. Data are expressed as the mean ± SD (n = 8). *, $p < 0.05$ and **, $p < 0.01$ significantly different from control; #, $p < 0.05$ and ##, $p < 0.01$ significantly different from model; &, $p < 0.05$ significantly different from CR-F_H. Yellow arrows represent vacuolar degeneration or necrotic shedding, red arrows represent inflammatory cell infiltration.

roles in steroid hormone biosynthesis, the estrogen signaling pathway, and the inflammatory response, all of which align closely with the pathological mechanisms underlying dysmenorrhea.

Notably, while CR-F significantly improved key biochemical markers of pain and inflammation, including 5-HT, β-EP, $PGF_{2\alpha}$, 6-Keto-$PGF_{1\alpha}$, and oxidative stress indices, no significant difference was observed in writhing frequency or latency compared with CR-T. This discrepancy highlights the importance of multi-modal assessment when evaluating analgesic efficacy, as reported in previous natural product studies[33]. The writhing test is a well-established but relatively gross behavioral endpoint, subject to high variability from animal handling, stress responses, and individual pain sensitivity[34]. In contrast, biochemical indicators (5-HT, β-EP, prostaglandins, and oxidative stress indices) directly reflect the molecular and physiological mechanisms underlying pain and inflammation in the uterus. These biochemical changes often occur earlier and can be more sensitive indicators of drug action than behavioral readouts, which may require a larger sample size or more refined testing protocols to detect subtle differences.

Although this study did not directly assess the gene and protein expression levels of these targets, it systematically evaluated the downstream prostaglandin family parameters ($PGF_{2\alpha}$, PGE2, TXB2, and 6-Keto-$PGF_{1\alpha}$) and oxidative stress indices *in vivo*, which are key functional effectors regulated by ESR1 and PTGS2. The significant improvement in these indicators in the CR-F group corroborates that CR-F alleviates dysmenorrhea by modulating the estrogen-prostaglandin pathway, aligning well with our target predictions. In future research, we aim to further validate the mRNA and protein expression of ESR1 and other core targets to provide more direct molecular evidence.

Although molecular docking has predicted that the differential components exhibit strong binding affinity with key targets such as

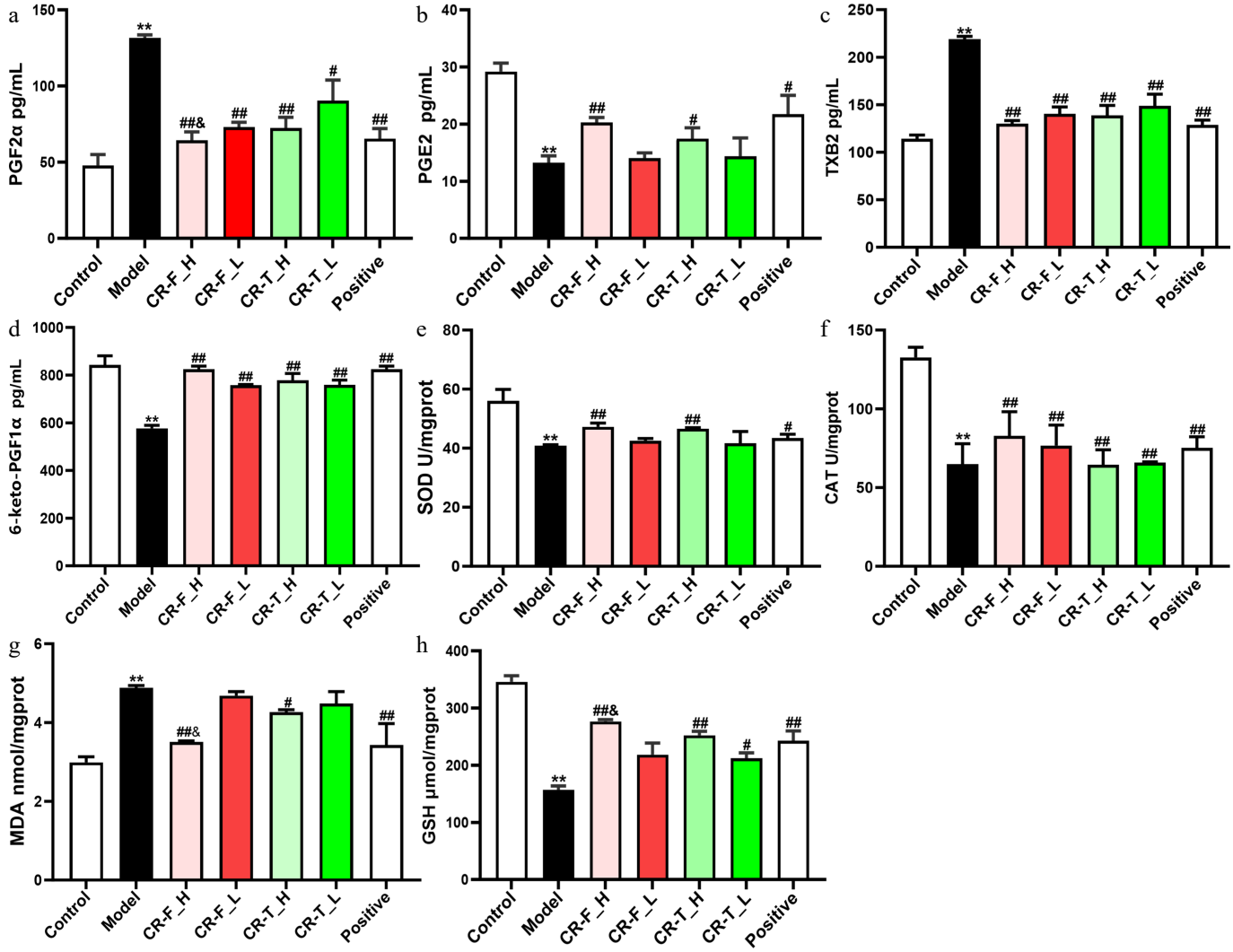

Fig. 8 The effects of CR-F and CR-T on biochemical indicators in the uterus of dysmenorrhea rats. (a) $PGF_{2\alpha}$, (b) PGE2, (c) TXB2, (d) 6-Keto-$PGF_{1\alpha}$, (e) SOD, (f) CAT, (g) MDA, (h) GSH. Data are expressed as the mean ± SD (n = 8). *, $p < 0.05$ and **, $p < 0.01$, significantly different from control; #, $p < 0.05$ and ##, $p < 0.01$, significantly different from model. &, $p < 0.05$ and &&, $p < 0.01$, significantly different from CR-T_H.

ESR1 and PTGS2, this study did not include *in vitro* activity verification or *in vivo* efficacy validation of these individual monomeric compounds. Consequently, it remains to be determined which monomer plays a decisive role in the anti-dysmenorrhea effect, and how multiple components may exhibit synergistic effects. Additionally, the regulatory mechanism by which fresh-cut processing influences the biosynthesis and accumulation of these alkaloid components has not been elucidated, representing a significant limitation of the current study. In future investigations, we plan to isolate and prepare the key monomeric compounds, conduct both *in vitro* and *in vivo* validations, identify the primary active components and their dose–effect relationships, and further examine the impacts of fresh-cut processing on component accumulation and the quality formation mechanism of CR. In addition, absolute quantitative determination with individual reference standards for the six differential alkaloids was not performed in the present study. Nevertheless, the standardized HPLC peak data combined with HCA and OPLS-DA analysis (VIP ≥ 1) as well as heatmap results revealed consistent relative enrichment of these six ingredients in CR-F among all tested batches. The validated fingerprint method and standardized sample collection effectively avoid random experimental errors, and the uniform changing trend can preliminarily confirm that fresh-cut processing is conducive to the retention of active ingredients. In the future, we will complete quantification to realize more intuitive data comparison.

Conclusions

The fresh cutting of Chinese medicinal materials minimizes the loss of active ingredients typically incurred through repeated processing, offering benefits such as reduced time, effort, and processing costs. This study established that the optimal moisture content range for freshly cut CR is between 35.95% and 44.52%. A quality comparison between CR-F and CR-T met the requirements of the pharmacopoeia, with CR-F exhibiting a higher retention rate of tetrahydropalmatine than CR-T. By concurrently identifying differences in six characteristic components using fingerprint technology and predicting pharmacological targets, it was determined that the fresh cutting and processing method of CR enhances its analgesic effect. This research provides theoretical support for the development of comprehensive and systematic quality standards for the

fresh cutting and processing of CR, and serves as a foundation for quality control and the standardized clinical use of CR medicinal materials.

Ethical statements

This study was approved by the Ethics Committee of Shaanxi Academy of Traditional Chinese Medicine (Approval No. NWU-AWC-20240601M; dated July 01, 2024). The research followed the 'Replacement, Reduction, and Refinement' principles to minimize harm to animals.

Author contributions

The authors confirm their contributions to this study as follows: Conceptualization: Yang H, Liu J; writing – original draft: Yang H; methodology: Yang H, Zheng N, Sun T; formal analysis: Yang H, Li Z; writing – review & editing: Yang H, Li B, Sun T; supervision: Li B, Liu J; data curation: Li Z, Zheng N; investigation and Resources: Zhao H; project administration: Zhang H, Sun T; funding acquisition: Zhang H. All authors reviewed the results and approved the final version of the manuscript.

Data availability

The datasets generated and/or analyzed in the current study are available from the corresponding author on reasonable request.

Acknowledgements

This work was supported by the National Inheritance Workshop for Old Medicine Workers of the State Administration of Traditional Chinese Medicine (No. [2024]255); the Shaanxi Department of Science and Technology Project (No. 2022SF-183); and the Shaanxi Provincial Administration of Traditional Chinese Medicine Project (2021-04; TZKN-CXRC-12). We thank the Shaanxi Innovative Healthcare Team for Qin Medicine Quality Control and Product Research and Development for their support.

Conflict of interest

The authors declare that they have no conflict of interest.

Supplementary information accompanies this paper online at: https://doi.org/10.48130/mpb-0026-0015.

Dates

Received 19 March 2026; Revised 7 June 2026; Accepted 9 June 2026; Published online 31 July 2026

References

[1] Tian B, Tian M, Huang SM. 2020. Advances in phytochemical and modern pharmacological research of Rhizoma Corydalis. *Pharmaceutical Biology* 58(1):265–275

[2] Zhang Y, Zhang W, Ma M, Zhang X, Li C, et al. 2025. *Corydalis yanhusuo* extract and its pharmacological substances alleviate food allergy by inhibiting mast cells activation *via* PLC/PKC/STAT3 pathway. *Journal of Ethnopharmacology* 337:118809

[3] Wu X, Tang S, Bian X, Ma Z, Zhang X, et al. 2025. Ethnomedicine, botany, phytochemistry, pharmacology, pharmacokinetics, and toxicity of *Rhizoma corydalis*: a systematic review. *The American Journal of Chinese Medicine* 53(5):1441–1476

[4] Feng JH, Chen K, Shen SY, Luo YF, Liu XH, et al. 2023. The composition, pharmacological effects, related mechanisms and drug delivery of alkaloids from Corydalis yanhusuo. *Biomedicine & Pharmacotherapy* 167:115511

[5] Alhassen L, Dabbous T, Ha A, Dang LHL, Civelli O. 2021. The analgesic properties of Corydalis yanhusuo. *Molecules* 26(24):7498

[6] Jin F, Tang Z, Song Z, Jiao H. 2025. 延胡索生物碱类化学成分及其提取分离、分析检测与药理活性研究进展 [Research progress on alkaloid chemical constituents of *Corydalis yanhusuo* and their extraction and separation, analysis and detection, and pharmacological activities]. *Natural Product Research and Development [天然产物研究与开发]* 38(3):648–661

[7] Kessler A, Kalske A. 2018. Plant secondary metabolite diversity and species interactions. *Annual Review of Ecology, Evolution, and Systematics* 49:115–138

[8] Liu S, Liu J, Li J, Xu Z, Lei K, et al. 2025. Quasi-targeted metabolomics analysis reveals linkage between chemical composition and different post-harvest processing methods of *Polygala tenuifolia*. *Medicinal Plant Biology* 4:e036

[9] Ni W, Zhou Z, Mao S, Li Z, Liu M, et al. 2026. Integrated metabolomics analysis of pigment metabolite accumulation and color development of fresh *Dendrobium officinale* juice after processing. *NPJ Science of Food* 10:162

[10] Sun X, Song Z, Tang Z, Yu J, Fan X, et al. 2025. Effects of different post-harvest processing methods on changes in the active ingredients of licorice based on LC-MS and plant metabolomics. *Phytochemical Analysis* 36(2):419–429

[11] Shi Y, Deng R, Deng X, Huang T. 2025. 白及的产地趁鲜切制工艺及可行性 [Fresh-cutting processing technology and feasibility of Bletilla striata]. *Hubei Agricultural Sciences [湖北农业科学]* 64(6):136–140

[12] Bai C, Yang J, Cao B, Xue Y, Gao P, et al. 2020. Growth years and post-harvest processing methods have critical roles on the contents of medicinal active ingredients of Scutellaria baicalensis. *Industrial Crops and Products* 158:112985

[13] Zhang A-S, Lin M, Duan G-H, Wu H-M, Wu Y-X, et al. 2023. 基于多质量参数的菝葜趁鲜切制工艺优选研究 [Optimization of fresh-cuting process of *Smilacis Chinae Rhizoma*]. *J Chinese Traditional and Herbal Drugs [中草药]* 54(12):3834–3841

[14] Wang S, Luo F, Yan M, Mahemuti A, Li J, et al. 2025. 管花肉苁蓉趁鲜蒸制工艺优化 [Optimization of steaming process for fresh *Cistanche deserticola*]. *Chinese Traditional Patent Medicine (中成药)* 48(6):2010–2015

[15] Qu Y, He J, Wang H, Yang Y, Li Z, et al. 2023. 黄丝郁金产地趁鲜加工关键技术与质量影响 [Key technology and quality influence of fresh processing in producing area of root tuber of *Curcuma longa* L.]. *China Journal of Traditional Chinese Medicine and Pharmacy [中华中医药杂志]* 38(9):4129–4135

[16] Xin E, Si X, Bian T, Niu J, Zhang Y, et al. 2020. Comparative study on the chemical composition between integral Comparative study on the chemical composition between integral. *West China Journal of Pharmaceutical Sciences* 35(5):505–508

[17] Xin X, Jing J, Gao S, Zhang J, Gong Q, et al. 2024. Analysis on Advantages of New Integration Processing Method in Producing Area of Polygoni Multiflori Radix Praeparata. *Chinese Journal of Experimental Traditional Medical Formulae* 30(8):167–175

[18] Zhang L, Zhang X, Begum N, Xia P, Liu J, et al. 2022. Effects of different processing methods based on different drying conditions on the active ingredients of *Salvia miltiorrhiza* bunge. *Molecules* 27(15):4860

[19] Zhang L, Zhang X, Liang Z. 2022. Post-harvest processing methods have critical roles in the contents of active ingredients of *Scutellaria baicalensis* Georgi. *Molecules* 27(23):8302

[20] Chinese Pharmacopoeia Commission. 2020. *Pharmacopoeia of the People's Republic of China* (2020 Edition). Beijing: China Medical Science Press. https://ydz.chp.org.cn/#/main

[21] Du W, Luo Y, Shi S, Li C, Ge W. 2019. 延胡索产地鲜切加工工艺响应面优化研究 [Optimization of response surface of fresh-cut processing technology in *Corydalis Rhizoma* producing area]. *Chinese Traditional and Herbal Drugs [中草药]* 50(5):1111–1116

[22] Xin E. 2020. *Study on process optimization and quality standard of rheum radix et rhizoma fresh-cut pieces*. Thesis. Gansu University of Chinese Medicine, China. doi: 10.27026/d.cnki.ggszc.2020.000080

[23] Zhang X, Jiao X, Su C, Luo Y, Zhang L, et al. 2023. Research progresses in and management strategies for aflatoxin contamination of fruits and seeds medicinal materials in China. *Plant Protection* 49(5):118−126

[24] Yao X, Xu M, Zhang X, Lu M, Liu X, et al. 2024. 甘草饮片趁鲜切制与传统切制方法对其质量的影响 [The influence of fresh cutting and traditional cutting methods on the quality of licorice slices]. *Journal of Chinese Medicinal Materials [中药材]* 47(2):342−347

[25] Yan Y, Lu L, Zhou Y, Wu Q, Wang S, et al. 2021. 川白芷产地趁鲜切制与传统切制方法对其质量的影响 [Effect of fresh cutting and traditional cutting methods on quality of *Angelica dahurica*]. *Chinese Traditional and Herbal Drugs [中草药]* 52(14):4176−4184

[26] Chen L, Zhang S, Chen R, Pu J, Zhang Y, et al. 2025. Influence of fresh-cut processing versus traditional processing on the components of the *Chaenomelis Fructus*. *Journal of Anhui University of Chinese Medicine* 44(6):94−100

[27] Wang S, Qian H, Liu C, Zhang G, Chen K, et al. 2024. Study on the optimization of processing technology of fresh cutting of *Aconiti Lateralis Radix* praeparata and comparison with traditional cutting. *Journal of Chinese Medicinal Materials* 47(10):2477−2484

[28] Zhang X, Jiang S, Sun T, Zhi W, Ding K, et al. 2024. Post-harvest processing methods have critical roles on the contents of active metabolites and pharmacological effects of *Astragali Radix*. *Frontiers in Pharmacology* 15:1489777

[29] Zhang G, Zhai H, Guo C, Song X, Zha L, et al. 2025. Quality assessment of fresh-cut dandelion medicinal material. *Journal of Anhui University of Chinese Medicine* 44(3):99−105

[30] Sun D, Gao H, Wang X, Yan L, Pang B. 2018. Antipyretic and anti-inflammatory effects of *Mosla chinensis* based on integration processing technology of origin. *Chinese Traditional and Herbal Drugs* 49(20):4737−4742

[31] Wu H, Li D, Song Q, Li G, Li X, et al. 2022. Comparative study on chemical composition and in vitro anti-oxidant activity of *Astragali Radix* fresh-cut pieces and traditional pieces. *Chinese Traditional and Herbal Drugs* 53(22):7039−7047

[32] Moshfegh F, Balanejad SZ, Shahrokhabady K, Attaranzadeh A. 2022. *Crocus sativus* (saffron) petals extract and its active ingredient, anthocyanin improves ovarian dysfunction, regulation of inflammatory genes and antioxidant factors in testosterone-induced PCOS mice. *Journal of Ethnopharmacology* 282:114594

[33] Liang W, Cao W, Zheng Y, Li T, et al. 2026. Integrated multi-omics elucidates the dual anti-inflammatory and neuroendocrine mechanisms of novel TCM plasters against primary dysmenorrhea. *Frontiers in Pain Research* 7:1727963

[34] Song Y, Ni J, Yuan J, Zhang Z, Wang D, et al. 2025. Effects of low-frequency and high-frequency electroacupuncture pretreatment on the COX-2/mPGES-1/PGE2 pathway in a rat model of cold-coagulation dysmenorrhea. *Frontiers in Immunology* 16:1563626